Inorganic crown: the host–guest chemistry of a high nuclearity 'Celtic-ring' isopolyoxotungstate $[H_{12}W_{36}O_{120}]^{12-}$†

De-Liang Long, Oliver Brücher, Carsten Streb and Leroy Cronin*

Received 9th November 2005, Accepted 2nd February 2006
First published as an Advance Article on the web 3rd May 2006
DOI: 10.1039/b515935k

A range of complexes based on the high-nuclearity $\{W_{36}\}$ isopolyoxotungstate cluster, $[H_{12}W_{36}O_{120}]^{12-}$, with a triangular topology has been isolated by using the organic cation, protonated triethanolamine. In analogy to an 18-crown-6 crown ether with six oxygen donors on a ring, the cluster can form alkali and alkaline earth metal complexes $\{M\subset W_{36}\}$ ($M = K^+$, Rb^+, Cs^+, NH_4^+, Sr^{2+} and Ba^{2+}, **1–6**, respectively). Compounds **1–6** were characterized by single-crystal X-ray diffraction, elemental analysis, IR spectroscopy. Comparisons between the structures of **1–6** and 18-crown-6 as well as the symmetry directing influence of the organo-cations in the isolation of the overall cluster architecture are discussed.

Introduction

The self-assembly of clusters based on molybdenum, tungsten or vanadium oxo anions gives rise to an almost unrivalled range of polyoxometalate cluster anions. The versatile nature of these clusters originates from the ability to polymerize metal-based polyhedra to form a range of clusters from low to high nuclearities.[1] In particular, the ability for molybdenum- and tungsten-based systems to form very large clusters has been demonstrated by a number of nano-sized cluster systems with over 100 tungsten[2] and molybdenum[3,4] atoms in a single cluster molecule. Therefore it is not surprising that polyoxometalates have been subjected to a vast number of studies due to their attractive electronic and molecular properties that give rise to a variety of applications *e.g.* in catalysis,[5,6] magnetism,[7,8] redox chemistry,[9,10] medicine,[11,12] and materials science.[13–15] Despite this great range of cluster types and properties, the ability to assemble large cluster systems from smaller known building blocks in a pre-determined way is a great challenge, as such routes could be a direct way to systematically control the overall cluster architecture and properties. This is because the understanding and manipulation of the self assembly processes that underpin the formation of POM clusters has to be an attractive route to enable the design of designer clusters and multi-functional materials, which take advantage of the unique physical properties associated with this extraordinary class of molecules.[1]

The true enormity of this challenge can be further clarified when one realizes the main route to synthesize POM clusters (large or small) often employs 'one-pot' reactions.[1–4] Therefore, the manipulation of some of the many reaction parameters often represents a straight-forward, but rather tedious, route to new, self-assembled POM architectures. To overcome such problems, the design of larger architectures (based on clusters) using POM building blocks as synthons could provide a step change in the design and assembly of such systems. This is because the ability to assemble large cluster systems from smaller known building blocks could be a direct way to systematically control the overall cluster architecture and properties while retaining the geometries of the building blocks. Thus, such building blocks of well-defined shape and connectivity might form the basis for work towards the growth of nanoscopic clusters of predetermined structure and function.[16] However, the major problem with this approach lies in establishing routes to produce reactive building blocks present in solution in significant concentrations that can be reliably utilized in the formation of larger architectures, without re-organizing or isomerization to other fragments. Access to such building blocks has been the major limitation in stepwise growth of W- and Mo-based POM clusters. Such limitations may be circumvented by adopting an approach that kinetically stabilizes the building block in solution, thereby effectively preventing its reorganization to other structure types.[17–21]

One possible route to this goal is to use bulky organic cations to isolate a new structure type by virtue of the cations used to 'encapsulate' the new building blocks, thereby limiting their reorganization to simpler structural types.[17–21] By trapping clusters during the self-assembly process it may be possible to restrain the cluster from reorganizing into other well-known structure types, see Fig. 1. Also, in many cases, synthetic strategies to W- and Mo-based cluster systems are guided by the fact that structures of polyoxomolybdate clusters are frequently derived from highly stable, low-nuclearity structural archetypes such as the O_h-symmetric Lindqvist[22] anion $[Mo_6O_{19}]^{2-}$ and the various

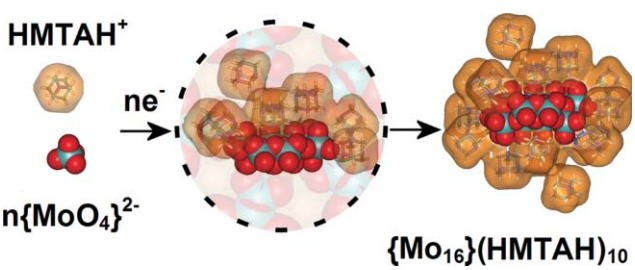

Fig. 1 A schematic showing the 'encapsulation' of the $[H_2Mo_{16}O_{52}]^{10-}$ cluster units during the cluster assembly process (shown schematically by the central view within the dotted circle) in the presence of the bulky organo-cation HMTAH (protonated hexamethylenetetramine).

WestCHEM, Department of Chemistry, The University of Glasgow, Glasgow, UK G12 8QQ. E-mail: L.Cronin@chem.gla.ac.uk

† Based on the presentation given at Dalton Discussion No. 9, 19–21st April 2006, Hulme Hall, Manchester, UK.

isomers of the Keggin structure,[23] $[M_{12}O_{36}(XO_4)]^{n-}$, or the Dawson structure,[24] $[M_{18}O_{46}(XO_4)_2]^{n-}$ (X = S, P, As, Si *etc.*) (M = W, Mo).[25]

Previously, by using protonated hexamethylenetetramine ($HMTAH^+$) as counter ions, we were able to stabilize and isolate a highly charged polyoxomolybdate anion, $[H_2Mo^{V}_4Mo^{VI}_{16}O_{52}]^{10-}$, $\{Mo_{16}\}$, which represents a new structural type.[17,18] The $\{Mo_{16}\}$ anion displays an unusual flat shape and can itself be formally decomposed into a highly condensed $\{Mo_{12}\}$ building block which incorporates two pairs of Mo^{V} centres and to which two edge-sharing $\{Mo_2\}$ groups are attached *via* corners. As we previously reported,[17,18] the $\{Mo_{16}\}$ is stable in the solid state as the salt $(C_6H_{13}N_4)_{10}[H_2Mo_{16}O_{52}]\cdot 34H_2O$ since the highly negative cluster anion is virtually completely wrapped by the organic $HMTAH^+$ cations. In an extension to this approach we also recently isolated a family of sulfite-based Dawson-type mixed-valence polyoxomolybdates $[Mo_{18}O_{54}(SO_3)_2]^{n-}$, using the same type of synthetic approach. Furthermore these $[Mo_{18}O_{54}(SO_3)_2]^{n-}$ clusters possess unusual electronic properties and display S···S interactions between the lone pairs of the two sulfite anions inside the cluster.[19] Thus, the use of bulky organic cations in the formation of Mo-based POMs appears to restrict aggregation to the more highly symmetrical cluster types, allowing a fundamentally more diverse set of clusters and cluster-based building blocks to be isolated, that display unprecedented structural[17,18] or physical[19] features. This observation was further explored by us when we used bulky organo-cations to rationally isolate and connect $\{Mo_8Ag_2\}$ building blocks to larger polymeric architectures.[21]

In previous work we showed that this simple but very efficient strategy can successfully be extended to polyoxotungstate chemistry, where we were able to isolate a $\{W_{36}\}$-based cluster. This has the formula $\{(H_2O)_4K\subset[H_{12}W_{36}O_{120}]\}^{11-}$ and represents the largest isopolyoxotungstate so far discovered.[26] Interestingly, the centre of this "Celtic-ring" cluster has a metal oxo framework that resembles the 18-crown-6 ether and also shows main features of crown ethers, for instance the ability to bind different metal ions in the central cavity of the cluster, see Fig. 2. The $\{K\subset W_{36}\}^{11-}$ anion is approximately C_{3v}-symmetric with a Celtic ring-like shape, and comprises three $\{W_{11}\}$ cluster subunits linked together by three $\{W_1\}$ bridges (shown as the cyan coloured polyhedra in Fig. 2). The $\{W_{11}\}$ cluster consists of a ring of six basal W positions, an additional W position in the centre of this ring, and four apical W positions in a butterfly configuration. Every W centre has a distorted WO_6 octahedral coordination geometry with one terminal W=O (W–O ~1.70 Å) extending away from the cluster. Within the $\{W_{11}\}$ moieties, two protons form hydrogen bonds between the four central $\mu_{3/4}$-oxo ligands. The three bridging $\{W_1\}$ groups also display a distorted WO_6 octahedral coordination geometry, each sharing four bridging oxo ligands in the equatorial plane with the $\{W_{11}\}$ clusters; one $W{=}O_{term}$ (W–O ~1.70 Å) points to the central potassium ion and one water ligand ($W{-}OH_2$ ~2.20 Å) points outside the cluster. The potassium ion has a rather distorted coordination geometry and is coordinated by 10 oxygen atoms; four of these 10 are water ligands (K–O distances are in the range 2.75(2) and 3.03(2) Å) the other six are O_{term} ligands coming from the WO_6 moieties. The potassium ion is displaced slightly above the equatorial plane, formed by the six O_{term} ligands, with three water molecules coordinating from above (RHS inset on Fig. 2), and one below the equatorial plane (LHS inset on Fig. 2). Overall the coordination geometry of the potassium ion can be described as a distorted polyhedron with 10 vertices, 16 faces and 24 edges and can be considered to be a kind of distorted dipyramid.

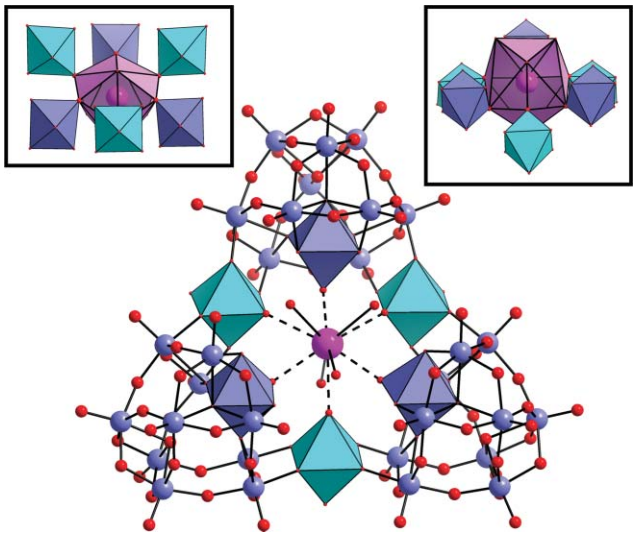

Fig. 2 Molecular structure of $\{(H_2O)_4K\subset[H_{12}W_{36}O_{120}]\}^{11-}$. The middle view shows a ball-and-stick representation of the W (blue) and O (red) framework. The central ten-coordinate K^+ ion is represented by a purple sphere. The K^+ ion is coordinated to the terminal oxygen positions of a $\{W_6O_6\}$ moiety (shown by the dotted lines) and each of these metal-centered polyhedra are shown in blue or cyan. Below, all the WO-based units interacting with the potassium ion are shown by polyhedral representations ($\{W_1\}$ linkers in cyan, and units from the $\{W_{11}\}$ fragments in blue). This view also reveals the "cavity" in which the K^+ ion resides. The top right inset shows the top view of the coordination around the potassium ion showing the trigonal face formed by the three coordinating water ligands on the front of the cluster. The top left inset shows the view from the bottom of the cluster with the single water ligand coordinated to the potassium ion.

It is interesting to see that the six WO_6 moieties, which form the cluster cavity in which the potassium ion is ligated, map extremely well onto the structure of the crown ether 18-crown-6. Using this observation as inspiration, we have extended our investigations to see how far this analogy can be taken. The present work extends this initial observation and focuses on the investigation of the host–guest chemistry of this new $\{W_{36}\}$ cluster by extending its potassium ion complex to other alkali and alkali-earth metal ions.[26]

Results and discussion

Synthesis of $\{W_{36}\}$ derivatives with alkali and alkali-earth metal cations

The $\{W_{36}\}$ cluster was initially isolated from an aqueous solution containing $NaWO_4\cdot 2H_2O$ and triethanolamine, which was adjusted to a pH of 2.0 with hydrochloric acid followed by the addition of $Na_2S_2O_4$ as reducing agent.[26] As revealed by X-ray crystallographic studies, the product has an approximate formula of $(TEAH)_9Na_2\{(H_2O)_4K\subset[H_{12}W_{36}O_{120}]\}\cdot 17H_2O$ (**1**). Although there was no potassium added to the reaction mixture, the X-ray crystallographic data clearly supports the unambiguous assignment of a K^+ ion coordinated to the central cavity of the cluster. Therefore the small amount of potassium needed to produce the cluster compound **1** was assumed to originate from

the glassware used. This assumption was confirmed by atomic absorption analysis on the postulated $\{K\subset W_{36}\}$ system, which indeed revealed the presence of potassium at the required concentration. The slow sequestration of potassium from the glassware was also supported by the observation that it took over four weeks for the product to form in the initial synthetic system, whereas the addition of potassium directly to the reaction mixture reduces this time to only a few days. Subsequent studies also demonstrated that no product was obtained when plastic flasks were used for the original reaction system. Furthermore the experiment confirmed that the addition of $Na_2S_2O_4$ is not necessary for the formation of the cluster **1**, although the addition of $Na_2S_2O_4$ can form a more soluble reduced polyoxotungstate at the starting point, and this serves to prevent precipitation of insoluble polymers. However we have now discovered that warming of the solution can also prevent precipitation of the intermediates whilst the pH is lowered to the crystallization pH for compound **1**.

Comparisons between the $\{W_{36}\}$ cluster anions, crown ether chemistry and other polyoxometalates

Today the design of highly sophisticated macrocycles based on polyethers, the crown ethers, is continuing to accelerate since their first discovery by Pederson in the mid-1960s.[27,28] This is because they are an extremely important class of molecules capable of recognition and binding of cations. They are able to form selective and stable complexes with various cations, most notably metal ions, and their selectivity as complexing agents results from the definite size of the crown cavity, which only accepts cations of comparable ionic radii. The well known 18-crown-6 ether for instance, has an estimated cavity radius of 2.6–3.2 Å and is most suitable for complexing K^+, NH_4^+ and Rb^+, but is also known to bind to other metal cations.[28] As such, the crown ethers find ubiquitous application from ionophores in cation sensing, to phase transfer catalysis in chemical synthesis, to chiral separators in chromatography to name but a few.[29–31]

During the last two decades chemists realized that the size selectivity, so effectively applied by crown ethers in the differentiation and complexation of cations, could also be utilized to recognize, design, and apply inorganic ring-type compounds that resemble organic crown ethers for binding cations. Notable examples are reported by Pecoraro *et al.* such as $[Mn_{11}(salicylhydroximate)]_4^{2-}$,[32] $[C_{45}H_{50}N_{10}O_{10}Cu_5Sm]$[33] and $[Cu^{II}(picha)]_5$ (picha = picoline hydroxamic acid),[34] which are often referred to as metallacrowns. This comparison may also be made with the $\{W_{36}\}$ cluster, which in analogy to 18-crown-6, has a very similar cavity radius of *ca.* 2.8 Å, see Fig. 3.

Polyoxometalates can also encapsulate metal ions such as potassium in a $\{W_{65}\}$ cluster,[35] and a $\{Mo_{80}V_{22}\}$,[36] but these do not involve a cavity that can be compared to classical crown ethers. However one novel compound, the Keplerate ball, reported by Müller *et al.*,[37] has a spherical framework with a high charge and accessible inner chamber. This cluster, of the form $\{Mo^{VI}{}_{72}Mo^{V}{}_{60}L_{30}\}^{n-}$ ($n = 42$ when L = acetate, $n = 72$ when L = sulfate) has been investigated as a type of 'inorganic-cell' whereby the cluster behaves as a semi-permeable inorganic membrane open for H_2O and small cations.[37] This is because the cavities, or pores shown in the Keplerate have the form $\{Mo_9O_9\}$ and provide a structural motif rather similar to that of the classical crown ethers.

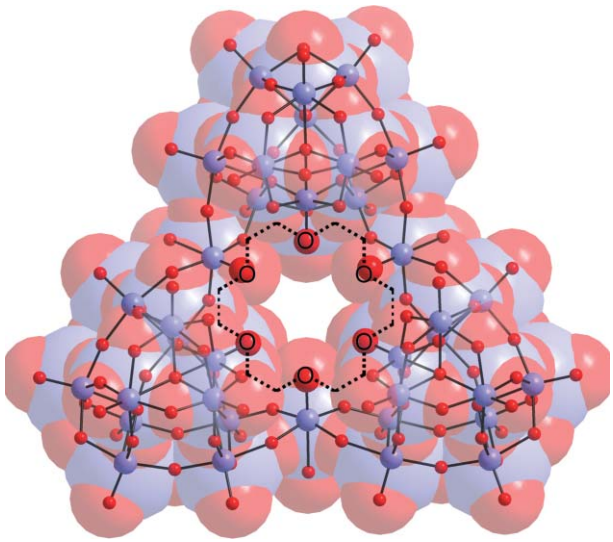

Fig. 3 Comparative illustration of the $\{W_{36}\}$ cluster framework and the 18-crown-6 structure (show to scale). W and O atoms shown as blue and red spheres with the crown ether superimposed on O atoms forming the 'cavity' of the cluster (these are larger for clarity). The ball and stick structure is also superimposed on the space-filling CPK representation of the $\{W_{36}\}$ to show the central cavity.

Complexes of $\{W_{36}\}$ with Rb^+, Cs^+, NH_4^+, Sr^{2+} and Ba^{2+}

As already discussed, the $\{W_{36}\}$-based cluster type has a similar oxygen coordination environment as in the 18-crown-6 ether and also shows the ability to capture potassium ions from aqueous solution, even though the oxygen atoms that comprise the 'crown-like' cavity are terminal oxo ligands rather than the bridging oxo ligands found in both organic-based crown ethers and the metallacrowns.[32–34] Extension of this work was relatively straightforward in so far as our experiments were conducted in plastic vessels (to avoid sequestration of potassium from glassware; the potassium originates from the KOH/alcohol base bath used to clean the glassware),[26] and the new metal cations added to the solution of the cluster at the correct pH. Interestingly, in the presence of only Na^+, the $\{W_{36}\}$ cluster could not be isolated, even if the concentration of Na^+, was elevated in the reaction mixture.

Therefore experiments, with Rb^+, Cs^+, NH_4^+, Sr^{2+} and Ba^{2+} were carried out as a function of pH, concentration of tungstate, triethanolamine and total ionic strength. By varying these parameters and adjusting an aqueous solution of sodium tungstate and triethanolamine hydrochloride to a certain pH with HCl solution, followed by a short period of heating, the corresponding chlorides of these cations were added to the reaction mixture which was then stored for crystallization. In addition to the use of plastic vessels, special attention was focussed on preventing possible contamination of the reactions with potassium sources (*e.g.* from the reagents, pH meter *etc*). As a further internal control, samples of the reaction mixtures, without added metal salt were kept as control samples and were never observed to lead to the formation of the $\{W_{36}\}$ cluster. This indicated that the potassium-free approach was efficient and the results of these investigations are shown below (Table 1).

During the reactions, the $\{W_{36}\}$ cluster emerged as colourless needles of $\{W_{36}\}$-based clusters **1–6** which were obtained for all

Table 1 Results from the formation of $\{W_{36}\}$ derivatives with K^+, Rb^+, Cs^+, NH_4^+, Sr^{2+} and Ba^{2+} chloride salts

Metal salt	pH	W/M$^+$ ratio	Yield (%)	Product formula
KCl	2.2	15 : 1	49	$(TEAH)_9Na_2\{(H_2O)_4K\subset[H_{12}W_{36}O_{120}]\}\cdot 17H_2O$ (**1**)
RbCl	2.2	15 : 1	39	$(TEAH)_9Na_2\{(H_2O)_4Rb\subset[H_{12}W_{36}O_{120}]\}\cdot 17H_2O$ (**2**)
CsCl	2.2	15 : 1	32	$(TEAH)_9Na_2\{(H_2O)_4Cs\subset[H_{12}W_{36}O_{120}]\}\cdot 15H_2O$ (**3**)
NH_4Cl	1.8	10 : 1	38	$(TEAH)_9Na_2\{(NH_4)\subset[H_{12}W_{36}O_{120}]\}\cdot 19H_2O$ (**4**)
$SrCl_2\cdot 6H_2O$	2.2	15 : 1	52	$(TEA)(TEAH)_8Na_2\{(H_2O)_4Sr\subset[H_{12}W_{36}O_{120}]\}\cdot 17H_2O$ (**5**)
$BaCl_2\cdot 2H_2O$	1.3	30 : 1	48	$(TEA)(TEAH)_8Na\{(H_2O)_4Ba_{1.5}\subset[H_{12}W_{36}O_{120}]\}\cdot 17H_2O$ (**6**)

of the applied cations. For K^+, Rb^+, Cs^+, NH_4^+, Sr^{2+}, the reaction condition with a pH of 2.2 seems to be optimal for the formation of the $\{W_{36}\}$ cluster, whereas for Ba^{2+} no crystals could be obtained (but material quickly precipitates from solution) at this pH value directly. Therefore the Ba^{2+} compound was produced as follows: the barium chloride was added to the tungstate solution at pH 1.3 and then the pH of the solution was brought up to 2.2 for crystallization. It would appear that a lower pH is needed for the $\{W_{36}Ba\}$-unit formation and then again a significant higher pH to allow crystallization. Further, although the ionic radii of the potassium- and the ammonium ion are almost the same, crystals from the $\{W_{36}NH_4\}$ cluster **4** were only obtained in lower yields and took a longer time to crystallize out.

Structures of compounds 2–6

The structures of all cluster derivatives **1–6** were determined by single-crystal X-ray diffraction. Except that **1** was previously reported,[26] crystal structures of **2–6** are included in this paper. All six compounds are essentially isomorphous and crystallize in the same orthorhombic system with space group *Pnma*. The asymmetric unit contains only half a $\{W_{36}\}$ cluster with a crystallographic mirror plane passing through the cluster and the central coordinated metal ions (K^+ to Ba^{2+}). Even though the $TEAH^+$, sodium cations and solvent water molecules are highly disordered, the main structures, *i.e.* the cluster anion $[H_{12}W_{36}O_{120}]^{12-}$ together with the coordinated metal ions K^+ to Ba^{2+}, are well defined. Compounds **2** $\{W_{36}Rb\}$ and **5** $\{W_{36}Sr\}$ incorporate Rb^+ and Sr^{2+} in the centre of the $\{W_{36}\}$ cavity at full occupancy as determined by crystallographic analysis, similar to the K^+ found in **1**, see Fig. 4. However, the NH_4^+ ion in **4** is disordered over two positions nearly half up the O_6 plane of the $\{W_{36}\}$ cluster and half down, see Fig. 4. In compound **3** $\{W_{36}Cs\}$, the Cs site at the centre of the $\{W_{36}\}$ cavity is not fully occupied and additional electron density that can be assigned as partially occupied Cs ion positions was found elsewhere between two $\{W_{11}\}$ cluster subunits, see Fig. 4.

These positions can only be assigned to partially occupied Cs centres according to the bond distances to neighbouring oxygen atoms. Interestingly, the $\{W_{36}Ba\}$ complex, compound **6**, shows some difference in the crystal structure to the other metal cation derivatives, see Fig. 4. As revealed by single-crystal X-ray diffraction and chemical analysis, this compound contains one and a half Ba^{2+} cations per cluster $\{W_{36}\}$ unit. The extra half Ba^{2+} cation was found to sit between $\{W_{36}\}$ frameworks and link them together to form 3-D polymers in the solid state, see Fig. 5. This observation also helps explain the poor solubility of compound **6** in water. While compound **3** $\{W_{36}Cs\}$ is the most soluble derivative, compound **6** is only about half as soluble. The decreased solubility of the latter can be explained with the stated linking of the cluster frameworks by the additional Ba^{2+} ions present in the structure. Interestingly, the terminal oxo ligands of the $\{W_{36}\}$

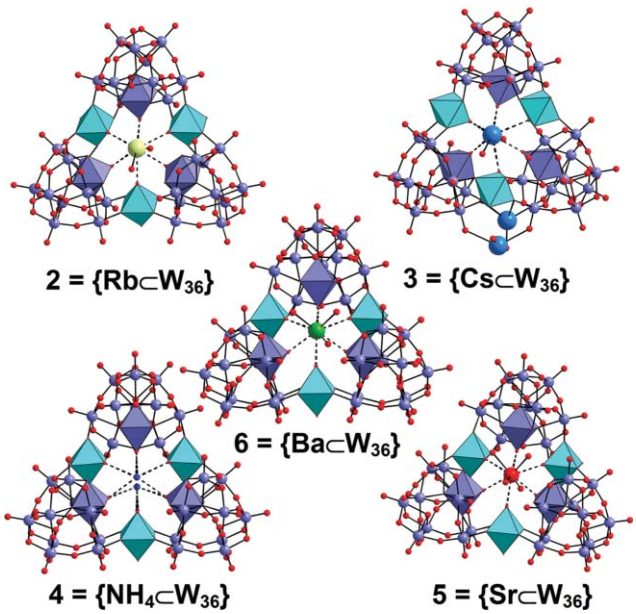

Fig. 4 Representations of the crystal structures of the $\{W_{36}\}$ framework complexed with Rb^+ (**2**), Cs^+ (**3**), NH_4^+ (**4**), Sr^{2+} (**5**) and Ba^{2+} (**6**). Colour scheme same as for Fig. 2 except the central complexed ions (Rb^+: pale green, Cs^+: blue, NH_4^+: small blue spheres, Sr^+: red, Ba^{2+}: green).

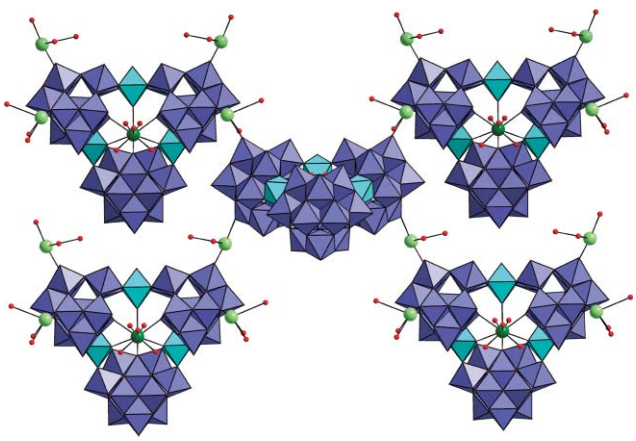

Fig. 5 Representation of the network formed in compound **6**. The $\{W_{36}\}$ is shown in polyhedral view ($\{W_{11}\}$-units-blue) with the linking $\{W_1\}$ units in cyan. The Ba^{2+} in the cavity are shown in dark green and those connecting the clusters light green. The coordinating water ligands are shown as red spheres.

cluster that are connected to the polymeric network by the Ba^{2+} were previously postulated (on the basis of DFT calculations[26]) as to be one of the possible sites (high nucleophilicity) for linkage with electrophiles.

Given the $\{W_{36}\}$ cluster has a triangular shape (this is unique among the known family of isopolyoxometalates, even though there are a few examples of triangular heteroPOMs, $[P_5Co_9W_{27}O_{119}H_{17}]^{16-}$,[38] $[(\alpha\text{-}SiW_{11}MnO_{38}OH)_3]^{15-}$.[39]), with the cavity centre resting on the approximate C_3-symmetry axis (Fig. 1), it is possible to examine the displacement of the complexed metal ions from the equatorial plane formed by the six terminal oxo-ligands. The degree of displacement from the equatorial plane above or below should reflect the increasing ionic radii of the cations as they fit less well into the cavity. These displacements are pronounced in the metal ion derivatives **1–3** and **4,5**, which can be seen in distances between the corresponding central ions and the six surrounding oxygen atoms from the W=O ligands of the $\{W_{36}\}$ crown. These distances are summarized in Table 2 and visualized in Fig. 6.

As seen in the table, the found average metal–oxygen distances in the $\{W_{36}\}$ host–guest complexes **1–6** are very close to those shown in the corresponding 18-crown-6 complexes. The metal cations in the synthesized compounds show different distances to the equatorial plane of the cluster framework which reflect the different sizes of their ionic radii, see Fig. 6.

Although there are some great similarities between the $\{W_{36}\}$ system and 18-crown-6, there are some features that are not common to both systems. Firstly the six-coordinated oxygen atoms on $\{W_{36}\}$ are not planar but in a manner with three oxo ligands up and three down alternatively forming two parallel planes distant at ~0.5 Å, while those on 18-crown-6 can adopt a planar conformation. Further, the $\{W{=}O\}_6$ donor groups of the $\{W_{36}\}$ crown are considerably more rigid unlike 18-crown-6, which is much more flexible. This means that 18-crown-6 can deform to form metal complexes with small ions like Na^+, Ca^{2+}, lanthanide ions and d-transition metal ions. This is because 18-crown-6, along with other similar crown ethers is able to distort and wrap itself around these smaller metal cations in an attempt to maximize the electrostatic interactions. This increases the strain of the ligand, which makes these complexes less stable than the ones with metal cations of optimal spatial fit. However, the $\{W_{36}\}$ framework, due to its high rigidity, simply cannot change conformation in such a way to bind these metal cations. This is partly confirmed by the observation that the diameter of the central cavity present in the family of $\{W_{36}\}$ clusters presented here is very well defined and shows no significant differences in structures **1–6**. In addition,

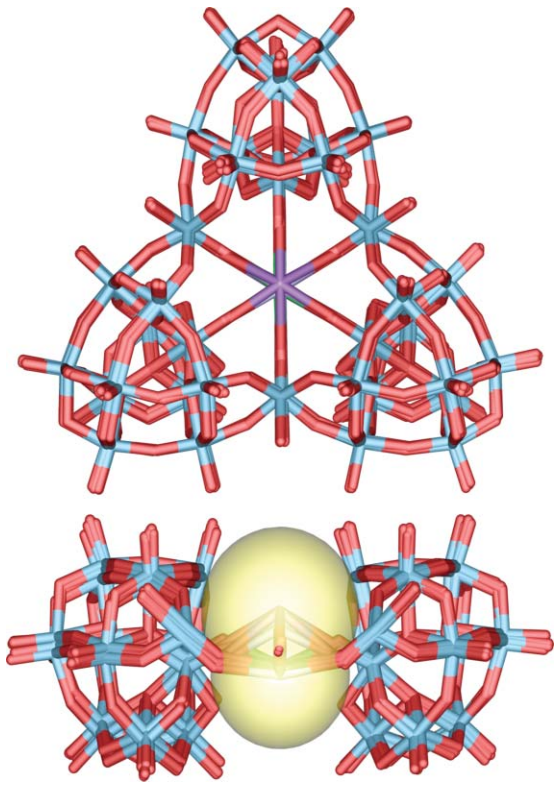

Fig. 6 An overlay of the six structures of **1–6**. The top view shows that the framework of $\{W_{36}\}$ is basically unchanged as a function of the cation complexed. The bottom view shows the maximum extent of the distortions found for all the complexes characterized; the largest distortions out of the plane upwards was found in compound **3** (Cs-surface in yellow) and downwards was found in compound **2** (Rb-surface in yellow). The front $\{W_{11}\}$ unit is omitted in the bottom side view for clarity.

other studies also confirmed that small ions cannot be complexed by the cavity present in the $\{W_{36}\}$ cluster. This is because we have attempted to synthesize the $\{W_{36}\}$ cluster in the presence of Ca^{2+}, lanthanide ions, and first row transition metal ions without success. Although experiments with $CaCl_2$ also yielded in colourless crystals, the presence of the Ca^{2+} ion in the cluster cavity could not be confirmed and chemical analysis showed only a low concentration of Ca^{2+} to be present in the system. In the case of lanthanide ions, the electrophilic nature of these cations appeared to complex rapidly with other tungstate-based species yielding polymeric compound precipitates rapidly upon reaction.

Table 2 Comparison of acquired metal-oxygen distances and displacements of metal ions to the cavity centre in the $\{W_{36}\}$ cluster and the corresponding figures for the 18-crown-6 ether (esds are all within 0.02 Å)

M^{n+}	Ionic radius/Å	Av. $d_{M\text{-}O}$[a] /Å ($\{W_{36}\}$ cluster)	Av. $d_{M\text{-}O}$/Å (18-crown-6)	$d_{M\text{-}c}$[b] /Å ($\{W_{36}\}$ cluster)	$d_{M\text{-}c}$/Å (18-crown-6)
K^+	1.38	2.80	2.80	0.70	0
Rb^+	1.52	2.87	2.95	0.84	0.93
Cs^+	1.67	3.16	3.18	1.61	1.47
Sr^{2+}	1.18	2.70	2.73	0.53	0
Ba^{2+}	1.35	2.82	2.82	0.73	0

[a] Av. $d_{M\text{-}O}$ is the average distance from M^{n+} to the six oxo ligands on the ring. [b] $d_{M\text{-}c}$ is the distance from M^{n+} to the cavity centre, which is defined as the intersection of the main molecular axis and the equatorial plane defined by the six oxo ligands.

pH and symmetry transferring effects on cluster formation

In our work we have been investigating the formation of new POM cluster types using a number of control parameters, in particular pH, and cation types, and have identified a very strong dependence upon both parameters. Indeed, there have been a number of reports that discuss the syntheses of a range of isopolyoxotungstates where the structural types are precisely controlled by the pH.[40–46] However there is no system reported previously concerning the uses of water-soluble organic cations to help isolation of new isopolyoxotungstates.

By using $TEAH^+$ cations, we have also isolated a number of heteroPOM Keggin ions and $[H_2W_{12}O_{40}]^{6-}$, as well as the $\{W_{36}\}$ (see in ref. 26) and a new isopolyoxotungstate $[H_4W_{19}O_{62}]^{6-}$.[47] The pH effects on cluster formation in the presence of $TEAH^+$ cations are summarized in Scheme 1. At pH around 4, the reaction always gives rise to the production of Keggin anion $[H_2W_{12}O_{40}]^{6-}$ as main product, however at a lower pH of *ca.* 2.0, the Keggin ion, $[H_2W_{12}O_{40}]^{6-}$, can also be produced as a by-product as well as the main $[H_{12}W_{36}O_{120}]^{12-}$ product. Of relevance to the work reported here, is that all the $\{W_{36}\}$-based complexes, **1–6** ($[H_{12}W_{36}O_{120}]^{12-}$), can only be produced at pH around 2.0 and the yields can be increased if the solution is warmed to dissolve the intermediate tungstate precipitates before the addition of the metal ions. By going to even lower pH values, and by refluxing for longer time, the system produces another new isopolyoxotungstate $[H_4W_{19}O_{62}]^{6-}$,[47] which has a Dawson-like structure of three-fold symmetry but with a $\{WO_6\}$ as central template rather than two hetero-tetrahedral $\{XO_4\}$ templates.

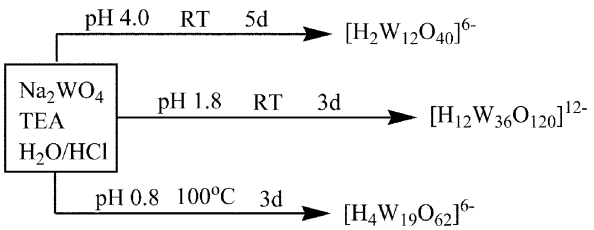

Scheme 1 pH effects in the synthesis of new POM clusters with TEA.

One extremely interesting observation we have made in all the work done utilizing the $TEAH^+$ cations, is that clusters with three-fold symmetry are exclusively produced from the reaction systems. These observations may be entirely circumstantial, but we have isolated over four distinct structure types using the $TEAH^+$ cations, and this has led us to propose that the $TEAH^+$ cation is able to transfer its symmetry onto the clusters in solution, see Scheme 2. Indeed, supramolecular interactions between the $TEAH^+$ cation and the cluster building blocks *via* the three hydroxyl groups on the $TEAH^+$ cation, can form H-bonds to intermediate components of the final product and possibly even guide their assembly to the overall cluster architecture. The first example we discovered was in the synthesis of reduced molybdosulfite cluster $[Mo_{18}O_{54}(SO_3)_2]^{6-}$, which was produced by the reaction of sodium molybdate with $Na_2S_2O_4$ reducing agent in the presence of TEA at a pH of *ca.* 4.[19] The cluster anion $[Mo_{18}O_{54}(SO_3)_2]^{6-}$ has a Dawson-like structure with main symmetry of a three-fold axis, which is therefore postulated to be derived from the templating influence of the three-fold symmetric $TEAH^+$ cation. Although appealing, we treated this idea with a degree of scepticism but

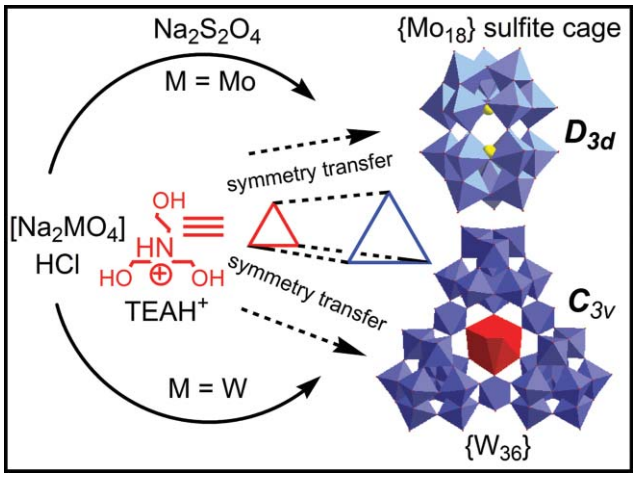

Scheme 2 The proposed symmetry transfer process, from the organo-cation to the cluster architecture *via* supramolecular interactions in solution, which allow the isolation of the new cluster type $\{Mo_{18}\}$[19] and $\{W_{36}\}$[26] with the same symmetry as the cation.

this hypothesis is strengthened further by the observation that similar reaction conditions (*e.g.*, pH value, concentrations, ionic strength, and temperature), but with different large cations, *e.g.* protonated hexamethylenetetramine, results in the formation of low symmetrical-type POM clusters of $[H_2Mo_{16}O_{52}]^{10-}$.[17,18] In the tungsten system, the observations of the cluster formation in $(TEAH)_6[H_2W_{12}O_{40}]$ at pH 4,[26] and $(TEAH)_6[H_4W_{19}O_{62}]$[47] at pH 0.8 also verify the symmetry-transferring hypothesis as these two clusters also demonstrate three-fold symmetry. Finally, the $\{W_{36}\}$ clusters shown in this paper all comprise three $\{W_{11}\}$ cluster subunits linked together by three $\{W_1\}$ bridges to form the overall triangular shaped cluster. However, the three $\{W_{11}\}$ subunits are analogous to the framework geometry of the $[H_4W_{11}O_{38}]^{6-}$ cluster, which was isolated by Lehmann *et al.* in the 1980s by using K^+ as counter cations at pH 1.3.[45] This $[H_4W_{11}O_{38}]^{6-}$ cluster has a spherical shape with approximate mirror symmetry. Therefore, the isolation of $[H_4W_{11}O_{38}]^{6-}$ as K^+ salt suggests that in solution, the $\{W_{11}\}$ cluster is the precursor for the $\{W_{36}\}$ clusters and the isolation of $\{W_{36}\}$ only become possible when three-fold symmetric $TEAH^+$ cations are present; indeed attempts to assemble the $\{W_{36}\}$ cluster in the presence of other cations, but under the same reaction conditions, has not been possible.

Conclusions

A range of new complexes of the triangular $\{W_{36}\}$ cluster, $[H_{12}W_{36}O_{120}]^{12-}$ that incorporate cations within the central cavity complexed by six W=O pendant donor groups, have been characterized. These complexes demonstrate the $\{W_{36}\}$ can act like a type of inorganic "crown ether" with similar preferences to 18-crown-6, but with much greater rigidity, and therefore, potential to distinguish between different cations. The synthetic routes to the $\{W_{36}\}$ cluster, along with other clusters we have previously characterized, using the $TEAH^+$ cation imply a possible route to 'imprinting' or transferring symmetry from the organo-cation to the cluster architecture. In future work we will attempt to

exploit the rigid nature of the $\{W_{36}\}$ and attempt to determine selectivity for a range of metal ions, as well as attempt to build new architectures by complexation of rigid organo-amines with primary amino groups that can be bound in the cavity of the $\{W_{36}\}$ cluster. We will also attempt to extend our observation of apparent symmetry transfer between the organo-cations and the cluster type to gain access to new polyoxometalates structure types and symmetries.[47]

Experimental

General procedures

All reagents and chemicals were purchased from commercial sources and used without further purification. Infrared spectra were recorded as KBr disc using a Perkin-Elmer paragon 1000 PC or Nicolet Magna 550 series II FTIR spectrometer. Elemental analyses were carried with dried samples. It should be noted that there are differences between the analytical values determined and theoretical values calculated from crystallographic formula. This is because these compounds contain a large amount of solvent of crystallization and drying occurs very quickly. However these problems were minor and did not hinder the overall formula determination for the main cluster $\{W_{36}\}$ and the guest metal ions encapsulated.

Synthetic procedures

Synthesis of $(TEAH)_9Na_2\{(H_2O)_4K\subset[H_{12}W_{36}O_{120}]\}\cdot 17H_2O$ (1). $Na_2WO_4\cdot 2H_2O$ (2.00 g, 6.06 mmol) and triethanolamine-hydrochloride (2.5 g, 13.47 mmol) were dissolved in H_2O (50 ml) in a plastic flask and the solution was adjusted to a pH of 2.2 with 2.0 ml HCl (4 M). After heating the reaction mixture to 80 °C in a water bath for 30 min, 0.030 g (0.40 mmol) KCl were added to the hot solution and the mixture was cooled down without further stirring. The sample was stored undisturbed for crystallization, which yielded colourless needles of **1** in 2–3 days. The crystals were collected on a filter paper and dried. Yield 0.869 g (49% based on W). IR (KBr disk): ν/cm^{-1}: 3447, 1622, 1449, 1401, 1320, 1256, 1205, 1093, 1065, 950, 895, 780, 654, 419; UV/VIS (H_2O): $\lambda_{max} = 276$ nm (br sh, 0.34); elemental analysis: calc. for $C_{54}H_{198}KN_9Na_2O_{168}W_{36}$: C 6.26, H 1.93, K 0.38, N 1.22, Na 0.44, W 63.9% found: C 6.69, H 2.00, K 0.38, N 1.39, Na 0.45, W 61.7%.

Synthesis of $(TEAH)_9Na\{(H_2O)_4Rb\subset[H_{12}W_{36}O_{120}]\}\cdot 17H_2O$ (2). The same procedure as preparing **1**, with RbCl (0.048 g, 0.40 mmol) replacing KCl, yielded colourless needles of **2** in 2–3 days. Yield 0.695 g (39% based on W). IR (KBr disk): ν/cm^{-1}: 3443, 1620, 1449, 1404, 1321, 1255, 1203, 1093, 1065, 950, 894, 778, 656, 421; UV/VIS (H_2O): $\lambda_{max} = 276$ nm (br sh, 0.34); elemental analysis: calc. for $C_{54}H_{198}N_9Na_2O_{168}RbW_{36}$: C 6.23, H 1.92, N 1.21, Na 0.44, Rb 0.82, W 63.6%; found: C 6.96 H 1.64 N 1.35, Na 0.44, Rb 0.81, W 64.7%.

Synthesis of $(TEAH)_9Na_2\{(H_2O)_4Cs\subset[H_{12}W_{36}O_{120}]\}\cdot 15H_2O$ (3). The same procedure as preparing **1**, with CsCl (0.067 g, 0.40 mmol) replacing KCl, yielded colourless needles of **3** in 3–4 days. Yield 0.689 g (39% based on W). IR (KBr disk): ν/cm^{-1}: 3450, 1620, 1449, 1404, 1320, 1255, 1203, 1093, 1065, 950, 894, 781, 652, 431; UV/VIS (H_2O): $\lambda_{max} = 276$ nm (br sh, 0.34); elemental analysis: calc. for $C_{54}H_{194}CsN_9Na_2O_{166}W_{36}$: C 6.22, H 1.88, N 1.21, Na 0.44, Cs 1.28, W 63.5; found: C 6.93 H 1.58 N 1.34, Na 0.55, Cs 0.81, W 64.1%

Synthesis of $(TEAH)_9Na_2\{(NH_4)\subset[H_{12}W_{36}O_{120}]\}\cdot 19H_2O$ (4). $Na_2WO_4\cdot 2H_2O$ (2.00 g, 6.06 mmol) and triethanolamine hydrochloride (2.5 g, 13.47 mmol) were dissolved in H_2O (50 ml) in a plastic flask and the solution was adjusted to a pH of 1.8 with 2.5 ml HCl (4 M). After heating the reaction mixture to 80 °C in a water bath for 30 min, 0.027 g (0.50 mmol) NH_4Cl dissolved in 5 ml H_2O were dropped to the stirred hot solution and the mixture was cooled down without further stirring. The sample was stored undisturbed for crystallization, which yielded colourless needles of **4** in 4–5 days. The crystals were washed with cold water, collected by filtration and dried. Yield was 0.662 g (38% based on W). IR (KBr disk): ν/cm^{-1}: 3442, 1623, 1485, 1456, 1404, 1321, 1255, 1197, 1093, 950, 897, 781, 666, 414; UV/VIS (H_2O): $\lambda_{max} = 276$ nm (br sh, 0.34); elemental analysis: calc. for $C_{54}H_{198}N_{10}Na_2O_{166}W_{36}$: C 6.29, H 1.94, N 1.36, Na 0.45, W 64.2; found: C 6.92 H 1.66 N 1.37, Na 0.46, W 66.5%.

Synthesis of $(TEA)(TEAH)_8Na_2\{(H_2O)_4Sr\subset[H_{12}W_{36}O_{120}]\}\cdot 17H_2O$ (5). The same procedure as preparing **1**, with $SrCl_2\cdot 6H_2O$ (0.107 g, 0.40 mmol) replacing KCl, yielded colourless needles of **6** in 2–3 days. Yield 0.93 g (53% based on W). IR (KBr disk): ν/cm^{-1}: 3433, 1620, 1449, 1398, 1320, 1257, 1204, 1093, 1066, 953, 898, 779, 660, 416; UV/VIS (H_2O): $\lambda_{max} = 276$ nm (br sh, 0.34); elemental analysis: calc. for $C_{54}H_{197}N_9Na_2O_{168}SrW_{36}$: C 6.23, H 1.91, N 1.21, Na 0.44, Sr 0.84, W 63.6; found: C 6.76 H 1.58 N 1.29, Na 0.48, Sr 0.81, W 64.0%.

Synthesis of $(TEA)(TEAH)_8Na\{(H_2O)_4Ba_{1.5}\subset[H_{12}W_{36}O_{120}]\}\cdot 17H_2O$ (6). $Na_2WO_4\cdot 2H_2O$ (1.00 g, 3.03 mmol) and triethanolamine hydrochloride (1.25 g, 6.73 mmol) were dissolved in H_2O (35 ml) and the solution was adjusted to pH 1.3 with *ca.* 3 ml HCl (4 M). After heating the reaction mixture to 80 °C in a water bath for 30 min, $BaCl_2\cdot 2H_2O$ (0.025 g, 0.10 mmol) dissolved in H_2O (5 ml) were added to the hot solution. The pH was then immediately adjusted to 2.2 with a few drops of aqueous triethanolamine solution (3M) and the mixture was cooled down without further stirring. After a little amount of white precipitate was filtered off, the sample was stored undisturbed for crystallization, which yielded colourless needles of **7** in 2–3 days. The crystals were washed with cold water, collected by filtration and dried. Yield was 0.422 g (48% based on W). IR (KBr disk): ν/cm^{-1}: 3434, 1618, 1450, 1386, 1320, 1257, 1203, 1093, 1067, 956, 895, 778, 647, 436; UV/VIS (H_2O): $\lambda_{max} = 276$ nm (br sh, 0.34); elemental analysis: calc. for $C_{54}H_{198}Ba_{1.5}N_9O_{168}Na_1W_{36}$: C 6.17, H 1.89, N 1.20, Na 0.22, Ba 1.96; W 62.8 found: C 6.29 H 1.74 N 1.20, Na 0.45, Ba 2.1, W 60.1%.

NMR measurements

Compounds **1–6** show basically the same signals in ^1H NMR spectra. These comprise two triplets for the methylene protons of the surrounding $TEAH^+$ cations at 3.4–3.6 and 3.8–4.0 ppm, small singlets between 5.2–5.6 ppm, which belong to the six protons forming hydrogen bonds inside the W_{11} moieties and various small signals in the H_2O area, which can not be clearly assigned to the different types of water molecules present in the cluster framework.

Table 3 Crystallographic data collection, intensity measurements and structure refinement parameters for **2–6**

	2	**3**	**4**	**5**	**6**
Chemical formula	$C_{54}H_{198}N_9Na_2O_{168}RbW_{36}$	$C_{54}H_{198}CsN_9Na_2O_{166}W_{36}$	$C_{54}H_{198}N_{10}Na_2O_{166}W_{36}$	$C_{54}H_{197}N_9Na_2O_{168}SrW_{36}$	$C_{54}H_{197}Ba_{1.5}N_9NaO_{168}W_{36}$
M/g mol^{-1}	10412.26	10423.67	10308.8	10413.41	10508.81
Symmetry	Orthorhombic	Orthorhombic	Orthorhombic	Orthorhombic	Orthorhombic
Space group	*Pnma*	*Pnma*	*Pnma*	*Pnma*	*Pnma*
a/Å	27.3088(3)	26.8369(10)	27.0818(4)	27.5918(3)	27.3739(4)
b/Å	35.1380(4)	34.8568(13)	35.1386(4)	34.9442(3)	35.1269(6)
c/Å	21.2632(3)	21.0337(8)	21.2120(3)	20.7727(2)	20.9520(4)
V/Å^3	20403.7(4)	19675.9(13)	20185.7(5)	20028.5(3)	20146.6(6)
Z	4	4	4	4	4
D_c/g cm^{-3}	3.39	3.52	3.39	3.45	3.47
μ/mm^{-1}	20.55	21.25	20.53	20.96	20.86
F(000)	18608	18600	18424	18608	18748
Crystal size/mm	0.30 × 0.14 × 0.14	0.30 × 0.12 × 0.10	0.30 × 0.09 × 0.08	0.25 × 0.22 × 0.16	0.30 × 0.06 × 0.06
No. data measured	111232	79977	92755	96316	84809
No. unique data	15357	15583	15979	15960	17021
No. observed data	10618	11664	9561	11392	11213
No. variables	1121	1112	1170	1182	1097
$R1$	0.0460	0.0386	0.0474	0.0370	0.0652
$R2$ (all data)	0.1146	0.1013	0.1001	0.0838	0.1780
Goodness of fit, S	1.039	1.062	1.009	1.039	1.056
Maximum shift/error	0.002	0.002	0.003	0.002	0.005

The exact chemical shift values for the methylene groups of the $TEAH^+$ cations depend on the included metal ion and differ slightly.

Crystallographic structure determinations

Details of data collection procedures and structure refinements are given in Table 3. Single crystals of suitable size were attached to glass fibres using Fomblin YR-1800 oil, and mounted. Some samples suffered solvent loss, and were glued to the glass fibre under solvent and transferred as rapidly as possible to the cold stream of the Oxford Instruments Cryostream. All data were collected on a Nonius KappaCCD or Bruker Apex II CCD diffractometer, equipped with graphite monochromated X-radiation ($\lambda = 0.71073$ Å), running under the Collect software. The structures were solved by SHELXS-97.[48,49] Most of the non-hydrogen atoms were refined anisotropically. In some structures the hydrogen atoms on the $TEAH^+$ cations were refined using a riding model using the SHELXL HFIX instructions. In all other cases hydrogen atoms on the $TEAH^+$ cations were not present due to disorders on the $TEAH^+$ cations themselves. No attempts were made to add hydrogen atoms to water molecules as they are quite disordered and have partial occupancy in the structures. Refinement was with SHELXL-97 using full-matrix least squares on F^2 and all the unique data. All samples showed the presence of disordered solvent molecules. All calculations were carried out using the WinGX package[50] of crystallographic programs.

CCDC reference numbers 289116–289120.

For crystallographic data in CIF or other electronic format see DOI: 10.1039/b515935k

Acknowledgements

This work was supported by the Leverhulme Trust (London), The Royal Society, The University of Glasgow and the EPSRC. The EPSRC provided funds for the X-ray diffractometer. We would like to acknowledge Prof. A. Slavin (the University of St Andrews) for help with the preliminary analysis of compounds **5** and **6**.

References

1 L. Cronin, High Nuclearity Clusters: Iso and Heteropolyoxoanions and Relatives, in *Comprehensive Coordination Chemistry II*, vol. 7, ed. J. A. McCleverty and T. B. Meyer, Elsevier, Amsterdam, 2004, pp. 1–56; M. T. Pope and A. Müller, *Angew. Chem., Int. Ed. Engl.*, 1991, **30**, 34; C. L. Hill, *Chem. Rev.*, 1998, **98**, 1.
2 K. Wassermann, M. H. Dickman and M. T. Pope, *Angew. Chem., Int. Ed. Engl.*, 1997, **36**, 1445.
3 L. Cronin, C. Beugholt, E. Krickemeyer, M. Schmidtmann, H. Bögge, P. Kögerler, T. K. K. Luong and A. Müller, *Angew. Chem., Int. Ed.*, 2002, **41**, 2805.
4 A. Müller, E. Beckmann, H. Bögge, M. Schmidtmann and A. Dress, *Angew. Chem., Int. Ed.*, 2002, **41**, 1162.
5 I. V. Kozhevnikov, *Chem. Rev.*, 1998, **98**, 171.
6 J. T. Rhule, W. A. Neiwert, K. I. Hardcastle, B. T. Do and C. L. Hill, *J. Am. Chem. Soc.*, 2001, **123**, 12101.
7 A. Müller, M. Luban, C. Schröder, R. Modler, P. Kögerler, M. Axenovich, J. Schnack, P. Canfield, S. Bud'ko and N. Harrison, *ChemPhysChem*, 2001, **2**, 517.
8 A. Müller, P. Kögerler and A. W. M. Dress, *Coord. Chem. Rev.*, 2001, **222**, 193.
9 D. M. Way, A. M. Bond and A. G. Wedd, *Inorg. Chem.*, 1997, **36**, 2826.
10 P. J. S. Richardt, J. M. White, P. A. Tregloan, A. M. Bond and A. G. Wedd, *Can. J. Chem.*, 2001, **79**, 613.
11 K. F. Aguey-Zinsou, P. V. Bernhardt, U. Kappler and A. G. McEwan, *J. Am. Chem. Soc.*, 2003, **125**, 530.
12 D. A. Judd, J. H. Nettles, N. Nevins, J. P. Snyder, D. C. Liotta, J. Tang, J. Ermolieff, R. F. Schinazi and C. L. Hill, *J. Am. Chem. Soc.*, 2001, **123**, 886.
13 H. D. Zeng, G. R. Newkome and C. L. Hill, *Angew. Chem., Int. Ed.*, 2000, **39**, 1772.
14 F. Ogliaro, S. P. de Visser, S. Cohen, P. K. Sharma and S. Shaik, *J. Am. Chem. Soc.*, 2002, **124**, 2806.
15 D.-L. Long, H. Abbas, P. Kögerler and L. Cronin, *Angew. Chem., Int. Ed.*, 2005, **44**, 3415.
16 P. Kögerler P and L. Cronin, *Angew. Chem., Int. Ed.*, 2005, **44**, 844.
17 D.-L. Long, P. Kögerler, L. J. Farrugia and L. Cronin, *Angew. Chem., Int. Ed.*, 2003, **42**, 4180.
18 D.-L. Long, P. Kogerler, L. J. Farrugia and L. Cronin, *Dalton Trans.*, 2005, 1372.
19 D.-L. Long, P. Kögerler and L. Cronin, *Angew. Chem., Int. Ed.*, 2004, **43**, 1817.
20 D.-L. Long, P. Kögerler, D. Orr, G. Seeber, L. J. Farrugia and L. Cronin, *J. Cluster Sci.*, 2003, **14**, 313.
21 H. Abbas, A. L. Pickering, D.-L. Long, P. Kögerler and L. Cronin, *Chem. Eur. J.*, 2005, **11**, 1071.

22 D. Hagrman, P. J. Hagrman and J. Zubieta, *Angew. Chem., Int. Ed.*, 1999, **38**, 3165; S. S. Kuduva, N. Avarvari and M. Fourmigue, *J. Chem. Soc., Dalton Trans.*, 2002, 3686.
23 P. Mialane, A. Dolbecq, L. Lisnard, A. Mallard, J. Marrot and F. Secheresse, *Angew. Chem., Int. Ed.*, 2002, **41**, 2398.
24 T. Hori, O. Tamada and S. Himeno, *J. Chem. Soc., Dalton Trans.*, 1989, 1491; S. Juraja, T. Vu, P. J. S. Richardt, A. M. Bond, T. J. Cardwell, J. D. Cashion, G. D. Fallon, G. Lazarev, B. Moubaraki, K. S. Murray and A. G. Wedd, *Inorg. Chem.*, 2002, **41**, 1072.
25 M. T. Pope, in *Comprehensive Coordination Chemistry*, ed. G. Wilkinson, R. D. Gillard and J. A. McCleverty, Pergamon Press, Oxford, 1987, vol. 3.
26 D.-L. Long, H. Abbas, P. Kögerler and L. Cronin, *J. Am. Chem. Soc.*, 2004, **126**, 13880.
27 C. J. Pedersen, *J. Am. Chem. Soc.*, 1967, **89**, 7017.
28 C. J. Pedersen, *Fed. Proc.*, 1965, **27**, 1305.
29 C. L. Liotta and H. P. Harris, *J. Am. Chem. Soc.*, 1974, **97**, 224.
30 A. P. d. Silva, H. Q. Gunaratne, T. Gunnlaugsson, A. J. Huxley, C. P. McCoy, J. T. Rademacher and T. E. Rice, *Chem. Rev.*, 1997, **97**, 1515.
31 M. H. Hyun and S. C. Han, *J. Biochem. Biophys. Methods*, 2002, **54**, 235.
32 M. S. Lah and V. L. Pecoraro, *J. Am. Chem. Soc.*, 1989, **111**, 7258.
33 A. D. Cutland-Van Noord, J. W. Kampf and V. L. Pecoraro, *Angew. Chem., Int. Ed.*, 2002, **41**, 4667.
34 A. J. Stemmler, J. W. Kampf, M. L. Kirk, B. H. Atasi and V. L. Pecoraro, *Inorg. Chem.*, 1999, **38**, 2807.
35 U. Kortz, M. G. Savelieff, B. S. Bassil and M. H. Dickman, *Angew. Chem., Int. Ed.*, 2002, **41**, 3384.
36 A. Müller, B. Botar, H. Bögge, P. Kögerler and A. Berkle, *Chem. Commun.*, 2002, 2944.
37 A. Müller, D. Rehder, E. T. K. Haupt, A. Merca, H. Bögge, M. Schmidtmann and G. Heinze-Brückner, *Angew. Chem., Int. Ed.*, 2004, **43**, 4466.
38 T. J. R. Weakley, *J. Chem. Soc., Chem. Commun.*, 1984, 1406.
39 U. Kortz and S. Matta, *Inorg. Chem.*, 2001, **40**, 815.
40 J. Fuchs, R. Palm and H. Hartl, *Angew. Chem., Int. Ed. Engl.*, 1996, **35**, 2651.
41 R. Bhattacharyya, S. Biswas, J. Armstrong and E. M. Holt, *Inorg. Chem.*, 1989, **28**, 4297.
42 H. Hartl, R. Palm and J. Fuchs, *Angew. Chem., Int. Ed. Engl.*, 1993, **32**, 1492.
43 J. Fuchs and E. P. Flindt, *Z. Naturforsch., Teil B*, 1979, **34**, 412.
44 Y. Sasaki, T. Yamase, Y. Ohashi and Y. Sasada, *Bull. Chem. Soc. Jpn.*, 1987, **60**, 4285.
45 T. Lehmann and J. Z. Fuchs, *Z. Naturforsch., TeilB*, 1988, **43**, 89.
46 I. Brüdgam, J. Fuchs, H. Hartl and R. Palm, *Angew. Chem., Int. Ed.*, 1998, **37**, 2668, and references therein.
47 D. L. Long, P. Kögerler, A. D. C. Parenty, J. Fielden and L. Cronin, *Angew. Chem., Int. Ed.*, 2006, submitted.
48 G. M. Sheldrick, *Acta Crystallogr., Sect. A*, 1998, **46**, 467.
49 G. M. Sheldrick, *SHELXL-97. Program for Crystal Structure Analysis*, University of Göttingen, Germany, 1997.
50 L. J. Farrugia, *J. Appl. Crystallogr.*, 1999, **32**, 837.

